J Mater Sci (2011) 46:715–722
DOI 10.1007/s10853-010-4799-3

Hydrogen-induced cracking susceptibility and hydrogen trapping efficiency of different microstructure X80 pipeline steel

F. Huang · X. G. Li · J. Liu · Y. M. Qu · J. Jia · C. W. Du

Received: 7 January 2010 / Accepted: 26 July 2010 / Published online: 28 August 2010

Abstract The hydrogen-induced cracking (HIC) susceptibility of the X80 steel in H_2S environment and its heated-treatment microstructure was evaluated. The field emission scanning electron microscopy (FE-SEM), high resolution transmission electron microscopy (HR-TEM) and energy dispersive spectroscopy (EDS) were employed to study the morphology and chemical composition of the inclusions, precipitates and HIC cracks in the X80 steel. The hydrogen trapping efficiency was investigated by measuring the permeability ($J_\infty L$) and the apparent diffusivity (D_{app}). The results showed that heat-treated specimens had lower trapping efficiency, but were more susceptible to HIC. Most of the HIC cracks initiated from the inclusions rich in Mn, Al, Ca, and Ti, and propagated transgranularly in the original and air cooled specimens, but mainly intergranularly in water quenched specimens.

Introduction

Petroleum and natural gas systems contaminated with aqueous H_2S are very corrosive to the steels used in petrochemical industries. Inspection programs indicate that 25% of equipment failures in the petroleum refining industry are in some way associated with the damage caused by hydrogen absorption, which takes place on the steels' surface by the corrosion reaction in aqueous H_2S environments [1]. When the hydrogen atoms penetrate into the steel and precipitate as hydrogen molecules at the matrix-inclusion interfaces, cracking may occur in low alloy steels, for pressure vessels and pipes, used in the oil and chemical industries. The embrittlement is often caused by the absorption of hydrogen due to the electrochemical reaction at the surface of steel [3, 4]. Two effects are generally provoked by the wet H_2S environments, hydrogen-induced cracking (HIC) and sulfide stress cracking (SSC) [1–6].

The presence of inclusions is an important factor affecting the HIC susceptibility. The susceptibility to hydrogen-induced cracking is closely related to the steel composition and the processing history because these parameters affect the formation of nonmetallic inclusions (type, size and morphology) and the material's ability to accommodate hydrogen. Large inclusions such as elongated manganese sulfides and stringers of oxide increase the HIC susceptibility [5]. Domizzi et al. [4] showed that the HIC susceptibility depended on the sulfur content, average length and total length per unit area of the sulfide inclusions.

HIC behavior depends not only on steel cleanliness but also on its microstructure [7, 8]. Boniszewski and Watkinson clearly demonstrated, from extensive work on the heat affected zones of welded steels, that both hardness and microstructure influence the susceptibility of low alloy steels to hydrogen embrittlement [4]. Cracking initiates and propagates more easily in the less ductile microstructures. Thus, segregated zones with bainitic or martensitic structures are harmful [6]. Carneiro et al. [1]

F. Huang · X. G. Li (✉) · C. W. Du
Corrosion and Protection Center, University of Science and Technology Beijing, Beijing 100083, China
e-mail: lixiaogang99@263.net

F. Huang · J. Liu · Y. M. Qu · J. Jia
College of Materials Science and Metallurgical Engineering, Wuhan University of Science and Technology, Wuhan, Hubei 430081, China

showed that the refined and homogeneously quenched and tempered bainite/martensite microstructure had the best performance against HIC and SSCC. On the other hand, other researchers found that acicular ferrite and ultrafine ferrite have the optimum HIC resistance as well as the good mechanical properties; the resistance against SSCC is better for acicular ferrite than for ultrafine ferrite [9]. Also, a non-quench ageing process was proposed to provide higher strength and better SSC resistance for acicular ferrite pipeline steels, without affecting their microstructures [10]. Park et al. [11] studied the effect of different microstructures on hydrogen-induced cracking of X65 pipeline steel. They found that acicular ferrite was the most efficient microstructure for hydrogen trapping, whereas the deformed pearlite was the least efficient.

The increasing tendencies toward operating under more severe environmental conditions and higher pressures have imposed demanding requirements for sour-resistant pipeline steels. The X80 steels are regarded as the most promising steel for high pressure gas pipeline applications in twenty-first century due to its high-strength and good ductility. In practice using, steel pipes are welded to form pipeline, and the microstructure at the weld joint zone may be adversely affected by the welding process, resulting in decrease in corrosion resistance, especially in wet H_2S environments. Du et al. [12] showed that in Ku'erle soil the corrosion rate of X70 steel with original microstructure was the lowest among the different microstructures obtained by water quenching, air cooling and furnace cooling. Microstructural hardening and grain coarsening increased SCC susceptibility of the X70 steel in simulating solutions of acidic soil in Yingtan in southeast China, and it was observed that hydrogen was actively involved in the SCC process [13]. Liu et al. [14] reported that two types of inclusions exist in the steel and play different roles in crack initiation. Nonetheless, the differences in HIC susceptibility and hydrogen diffusion in X80 steels between the base steel and the heat affected zones at the welds have not been examined in detail. Therefore, it is necessary to study the relationship between various microstructures and hydrogen diffusion in order to understand clearly the cracking problems induced by hydrogen.

One of the important research purposes for pipeline steels is to understand the corrosion behavior in relations to the complex microstructures resulting from welding procedures. Thus, the works are undertaken to evaluate the HIC resistance and hydrogen diffusion behaviors of X80 pipeline steels with different microstructures in wet H_2S environments. Nucleation and propagation of HIC cracks were investigated by taking into account of the effects of metallurgical factors such as microstructure and inclusions.

Experimental methods

Test material preparation and microstructure analysis

X80 pipeline steel used in this article was supplied by Wuhan Iron & steel Co., China, and its chemical composition was 0.041 wt% C, 1.67 wt% Mn, 0.010 wt% P, 0.003 wt% B, 0.196 wt% Si, 0.258 wt% Cu, 0.042 wt% Al, 0.011 wt% Ti, 0.031 wt% Cr, 0.246 wt% Ni, 0.095 wt% Nb with the Fe balance.

To conduct heat-treatment on the as received X80 steel (Marked as "steel O"), the specimens were held in a muffle furnace at 1,300 °C for 15 min to homogenize the structure, followed by air cooling (Marked as "steel A") or quenching in water (Marked as "steel W"). The quenched specimens were not tempered. The average cooling rate is approximately 10–30°/s for air-cooling and 200–400°/s for water quenching. The microstructures of the three specimens were analysed by means of multifunctional optical microscopy (Axioplan) and field emission-Scanning electron microscopy (FE-SEM) (Czechoslovakia Nova nano 400).

HIC susceptibility measurement

The NACE standard TM0284-2005HIC was used to evaluate the HIC susceptibility of the three specimens. The standard specimens size for the test was 20 mm × 100 mm × thickness, and the test was held at 25° for 96 h. The test solution, consisting of 0.5% acetic acid and 5% sodium chloride dissolved in distilled water, was saturated with H_2S. The original and final PH values of the solution were 2.72 and 3.83, respectively. After the test, the polished metallographical sections of each specimens were inspected for cracks. Three parameters for cracks were measured:

$$\text{Crack Length Ratio: CLR} = \frac{\sum a}{W} \times 100\% \quad (1)$$

$$\text{Crack Thickness Ratio: CTR} = \frac{\sum b}{T} \times 100\% \quad (2)$$

$$\text{Crack Sensitivity Ratio: CSR} = \frac{\sum (a \times b)}{W \times T} \times 100\% \quad (3)$$

where a is the crack length, b is the crack thickness, W is the section width, and T is the test specimen thickness.

After testing, the typical hydrogen-induced cracks were analyzed carefully using optical microscopy and FE-SEM linked to an Ametec EDS system in order to know the crack path and its correlation with the microstructure. In addition, the precipitates were analysed by Field Emission High-Resolution Transmission Electron Microscopy (FE-HRTEM) (JEM-2100F, Japan).

Hydrogen permeation test

The hydrogen diffusion behavior of X80 steels with different microstructures were investigated by the hydrogen permeation test, which was performed in a "modified Devanathan–Stachurski cell" [15] as shown in Fig. 1. Three specimens with different microstructures were prepared with an area of 20 × 20 mm^2 and thickness of 1.07 mm. Both sides of the specimens were polished to eliminate flux-limiting surface impedances and to ensure the reliability of the hydrogen oxidation current. The specimen was mounted between the two cells with a 1.00 cm^2 area exposed to each electrolyte in side cells. The deaerated 0.1 mol/L NaOH solution and the deaerated NACE TM028-2003 solution (a mixture of 5.0 wt% NaCl and 0.5 wt% glacial acetic acid dissolved in distilled water) saturated with H_2S, as same to HIC tests, were selected as test solutions in the hydrogen oxidation cell and the hydrogen charging cell, respectively. The potential of the steel membrane in the hydrogen oxidation cell was maintained at a potential of 250 mV_{SHE}, and the dominant oxidation reaction was oxidation of hydrogen which diffused through the steel membrane. During the hydrogen permeation test, H_2S gas was bubbled continuously through the NACE solution to maintain a positive pressure, and no potential was applied. Generally, the aqueous solution containing H_2S is highly corrosive, and it can corrode the surface of steel membrane in the hydrogen charging cell and form a sulfide scale, which may impede the hydrogen diffusion into the steel matrix. On the other hand, a relatively stable hydrogen permeation curve was obtained and corrosion occurred on the steel surface in the hydrogen charging cell during the test. Figure 2 illustrates the potential measured from the surfaces of the three X80 steels in the hydrogen charging cell. The potential

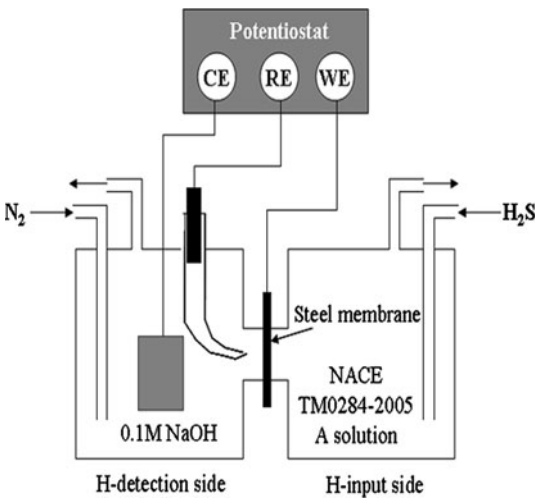

Fig. 1 Schematics of Modified Davanathan–Stachurski cell for hydrogen measurements

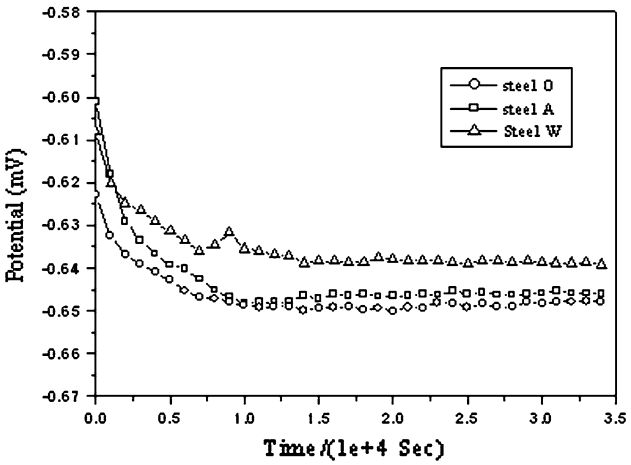

Fig. 2 Chang in potential of the steel membrane in the hydrogen charging cell with time during the permeation test.

during the test was maintained at about −650 mV_{SCE}, −645 mV_{SCE}, and −638mV_{SCE}, respectively, for original, air cooled, and water quenched samples, respectively; the pH value of the hydrogen charging solution changed from 2.76 to 2.81. In these potential and pH conditions, the Pourbaix diagram illustrates that the iron is immune to corrosion [11]. Although a limited degree of corrosion on the steel surface was observed after the test, it did not effect the hydrogen diffusion curves measured under the experimental conditions used.

The apparent hydrogen diffusivity in steels can be determined by the relaxation time, obtained from the hydrogen permeation curve [16]. The relationship between the steady-state current (I_∞), thickness of specimen (L), relaxation time (t_L), permeability ($J_\infty L$), apparent hydrogen diffusivity (D_{app}), and apparent hydrogen solubility (c_{app}) are related according to the following Eqs. 4–6:

$$J_\infty L = \frac{I_\infty L}{FA} \tag{4}$$

$$D_{app} = \frac{L^2}{6t_L} \tag{5}$$

$$c_{app} = \frac{J_\infty L}{D_{app}} \tag{6}$$

All experiments were performed at room temperature. In order to ensure the reliability of the experimental data, each test was repeated at least three times.

Results and discussion

Microstructure observation

The optical and scanning electronic microscopic images of the three specimens tested are shown in Fig. 3. For the

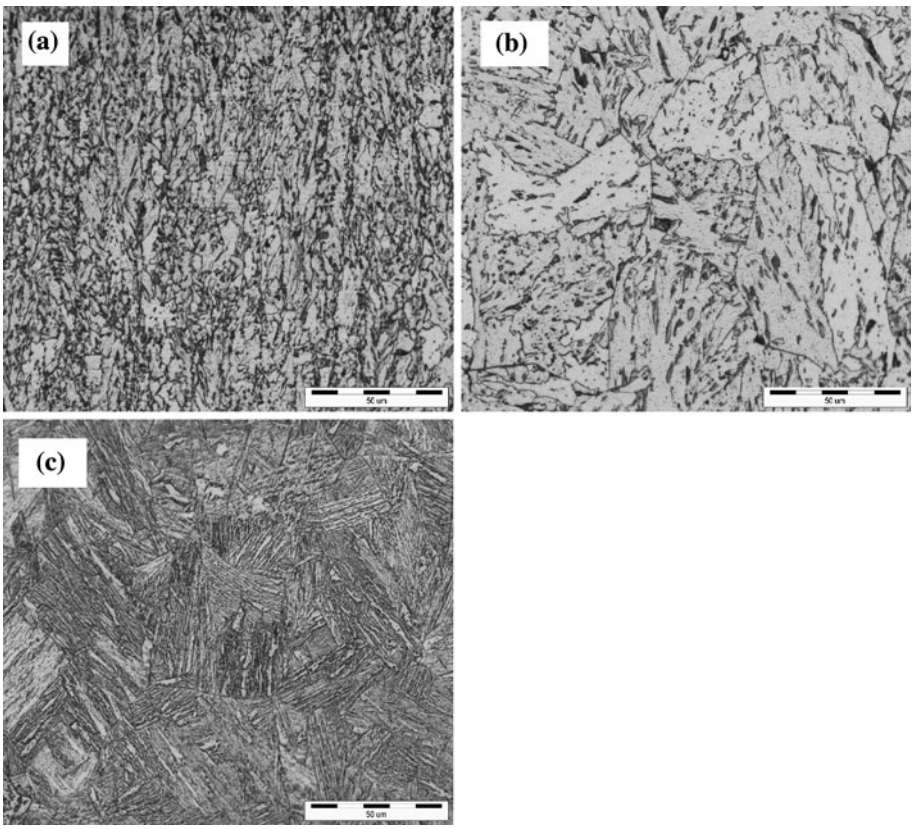

Fig. 3 Microstructures of X80 before and after heat treatment. **a** Original; **b** Air cooling; **c** Quchening

original specimen (Fig. 3a), fine acicular ferrite with irregular shape and martensite/austenite (M/A) islands were found diffusely distributed in grain and the grain boundary is incomplete. The microstructure of the air cooled specimen (Fig. 3b) consisted of polygonal ferrite and grain bainite, which grew from ferrite grain and sub-grain boundaries; and the size of ferrite was larger than that in original microstructure. The microstructure of the water quenched sample consisted of martensite and retained austenite (Fig. 3c). After heat treatment, the microstructure was coarser. It is accepted [12, 14] that water quenched microstructure is similar to the sclerosis microstructure near the fusion line of heat affected zone, and the air-cooled microstructure is similar to the softening microstructure.

HIC susceptibility

In general, both the HIC and SCC of the pipeline steels in H_2S environments are closely related to the hydrogen trapping. The most accepted corrosion reactions of steel exposed to wet H_2S gas are [15]:

Anodic reaction:

$$Fe \rightarrow Fe^{2+} + 2e \quad \text{(I)}$$

Dissociationreaction:

$$H_2S \rightarrow H^+ + HS^- \quad \text{(II)}$$

$$HS^- \rightarrow H^+ + S^{2-} \quad \text{(III)}$$

Cathodicreaction:

$$2H^+ + 2e \rightarrow 2H(\text{atomichydrogen}) \rightarrow H_2 \uparrow \quad \text{(IV)}$$

The hydrogen diffuses to the regions of high triaxial tensile stress or to some microstructural defects such as the inclusions and segregations and becomes trapped. When hydrogen pressure is up to a critical value, a crack will be initiated [7].

The values of CLR, CTR, and CSR for the three specimens tested are given in Table 1. No cracks were found in the crossed sections of the original specimen, when cracks were analyzed metallographically according to the NACE TM0284-2003 standard. These parameters were adopted as an acceptance criterion of HIC test for the other two heat-treated specimen. The water quenched specimen in which martensite were present suffered relatively larger susceptibility of HIC, compared with that of the air cooled specimen. The results implied that the X80 steel used in experiment and its deteriorated microstructure steels all had good HIC resistance in wet H_2S environment.

The HRTEM images of the three X80 specimens after HIC testing are presented in Fig. 4, which demonstrates that the precipitates were Ti, Nb(C, N) with a size in the range of 20–50 nm (Fig. 4d). After air cooling and water quenching, the size of the precipitates did not

Table 1 The HIC susceptibility parameters of the different microstructure X80 steel

Samples	Sections	CLR (%)	CTR (%)	CSR (%)
Original microstructure	1	0	0	0
	2	0	0	0
	3	0	0	0
	Average	0	0	0
Air cooling microstructure	1	0	0	0
	2	9.85	1.48	0.15
	3	0	0	0
	Average	3.28	0.49	0.05
Water quchening microstructure	1	0	0	0
	2	7.86	1.63	0.12
	3	13.02	1.3	0.17
	Average	6.96	0.98	0.096

change significantly, although the number of precipitates increased after air cooling. In addition, no HIC cracks were observed around the precipitates. Those results were accord with Zhao et al' investigation on the sulfide stress cracking (SSC) resistance of acicular ferrite (AF) and ferrite–pearlite (FP) in a microalloyed steel and in a non-microalloyed [17, 18]. Zhao et al. indicated that, in microalloyed steel, nano-sized carbonitrides were analyzed to behave as innocuous hydrogen traps, offering numerous sites for hydrogen redistribution and modifying, and should be attributed to the optimal SSC resistance of pipeline steels [17, 18]. All those indicated that the smaller sized precipitates cannot be the irreversible hydrogen trapping sites, and cannot induce cracks. In other words, the smaller sized precipitates did not affect HIC resistance of the X80 steels. It has been reported that the presence of inclusions is one of the dominant factors affecting the HIC [7, 15]. Heat-treatment could not influence the formation of inclusions, therefore the amount, size and distribution of inclusions in the three specimens tested remained almost the same. Taking into account all of the above factors, it was concluded that the difference in HIC resistance for the three specimens tested should be attributed to the difference in microstructure; the details will be discussed in fractography analysis and hydrogen measurement results.

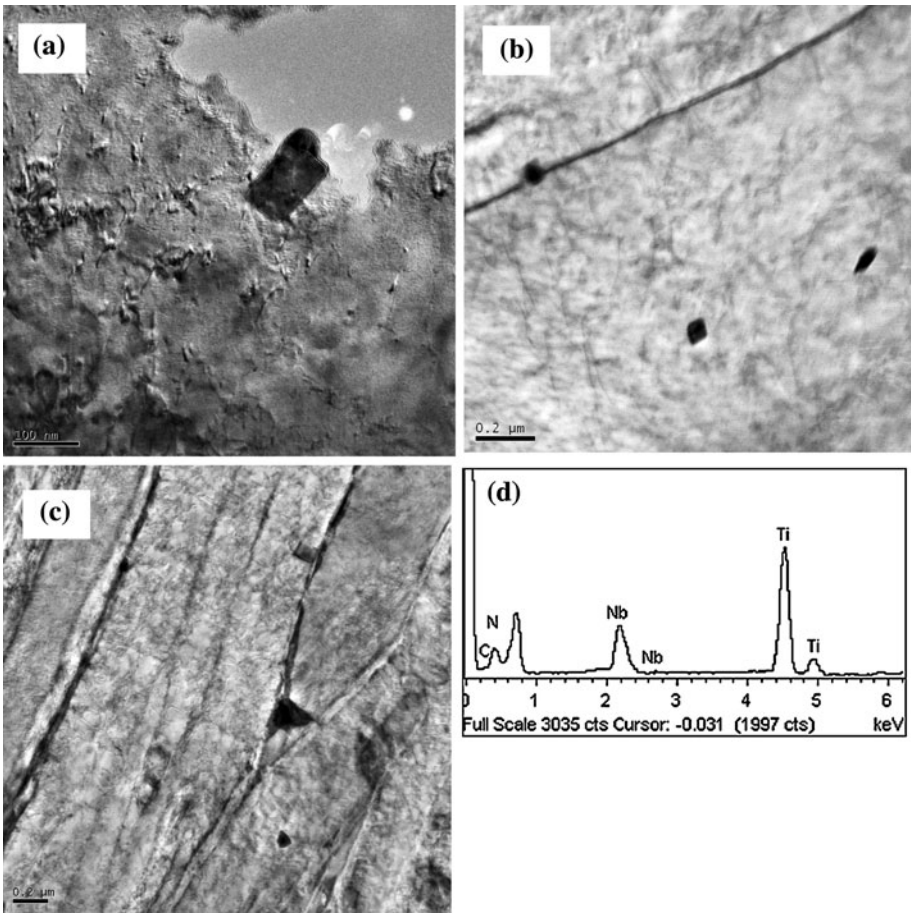

Fig. 4 The HRTEM images of the three microstructure of the X80 steels after HIC testing. **a** Original; **b** Air cooling; **c** Quchening

Hydrogen diffusion in X80 steels

The rate of hydrogen diffusion in steel is influenced mainly by two factors: one is the concentration of hydrogen at the steel surface, the other is the microstructure. Primary and secondary phases including non-metallic inclusions and precipitates can affect both the hydrogen trapping and diffusion in the steel. In this study, the deaerated NACE TM0284-2003 solution saturated with H_2S gas is used to simulate the practical environment of HIC measurement. There were slightly different in experimental procedures compared with the standard method [11].

The hydrogen diffusion through the steel membrane was assessed by the hydrogen permeation test. The D_{app}, $J_\infty L$, c_{app}, and amount of irreversibly trapped hydrogen were measured and calculated. The D_{app} represents the apparent lattice diffusivity of the dissolved and reversibly trapped hydrogen and the c_{app} corresponds to the hydrogen in the lattice and reversible traps [19]. It is often believed that the decrease in D_{app} and $J_\infty L$ and the increase in c_{app} indicate that more hydrogen can be trapped in steels.

It has have claimed that hydrogen is trapped into reversible and/or irreversible trap sites in steels [20]. If inclusions are considered only as irreversible trap sites in X80 steel, the amount of irreversibly trapped hydrogen in the three specimen tested would be almost the same because the similar inclusions were present in these steels. The amount of diffusible hydrogen is almost equal to that of the reversible hydrogen concentration in steels at room temperature. Therefore, the difference in the HIC resistance between the original X80 steel and those after different heat-treatments is due to the difference in the amount of diffusible hydrogen and reversibly trapped hydrogen.

The hydrogen permeation curves of the three specimens were determined in the NACE A solution saturated with H_2S as shown in Fig. 5. The calculated diffusion values of D_{app}, $J_\infty L$, and c_{app} are listed in Table 2, which shows that the air cooled and water quenched specimens had smaller D_{app}, $J_\infty L$ values and larger c_{app} values than the original specimen, the implication is that the lower the values of D_{app}, $J_\infty L$, and the larger the value of c_{app}, the more the hydrogen trapping occurs in the steel and the more the steels' susceptibility to HIC. In other word, more hydrogen can be trapped in the austenite/ferrite microstructure steel than in martensite microstructure.

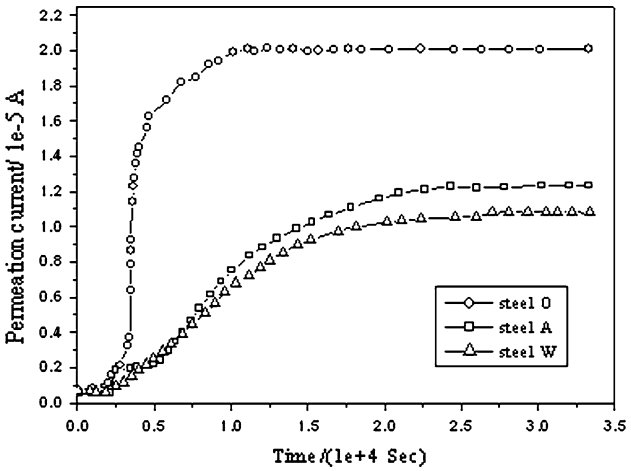

Fig. 5 Hydrogen permeation curve of the different microstructure X80 steel

Table 2 The hydrogen permeation data of different microstructure X80 steel

Parameters	Samples		
	Steel O	Steel A	Steel W
I_∞/(A)	2.01×10^{-5}	1.24×10^{-5}	1.08×10^{-5}
t_L/(s)	3,734	8,659	10,604
J_∞L/(mol·cm^{-1}·s^{-1})	2.1×10^{-11}	1.29×10^{-11}	1.09×10^{-11}
D_{app}/(cm^2·s^{-1})	5.11×10^{-7}	1.95×10^{-7}	1.59×10^{-7}
c_{app}/(mol·cm^{-3})	4.10×10^{-5}	6.61×10^{-5}	6.86×10^{-5}

HIC fractography observation and analysis

HIC cracks initiating

Figure 6 shows the BSE images of the surface of original, air cooled and water quenched specimens of X80 steel after HIC tests. It is seen that there were three types of inclusions in the steels, enriched in Mn (marked as A), or in Al (marked as B) or in Si (marked as C) as indicated by the EDS results in Fig. 6d, e, and f, respectively. The cracks initiated at or run across the inclusions A and B, but no cracks were initiated at the inclusion C, suggesting that the composition of the inclusion had a significant influence on HIC initiation. It is accepted [21] that inclusions rich in Al_2O_3 are hard, brittle and incoherent to the metal matrix. A quite big lattice deformation occurs near the inclusions. Consequently, interstices can be generated quite easily at the boundary between inclusions and metal. Moreover, hydrogen, once entered the steel, will prone to be trapped in these interstices, further developing into cracks [22]. Microvoids around MnS inclusions, caused by partial dissolution, could provide sites for hydrogen to accumulate, leading to crack initiation. In addition, the elongated MnS inclusions are regarded as temporary traps for hydrogen, encourage cracking in the hydrogen containing environments [22]. In general, inclusions rich in SiO_2 can be easily deformed, relieving effectively the residual stress. Moreover, SiO_2-rich inclusions are sphere shaped and relatively small local lattice deflection

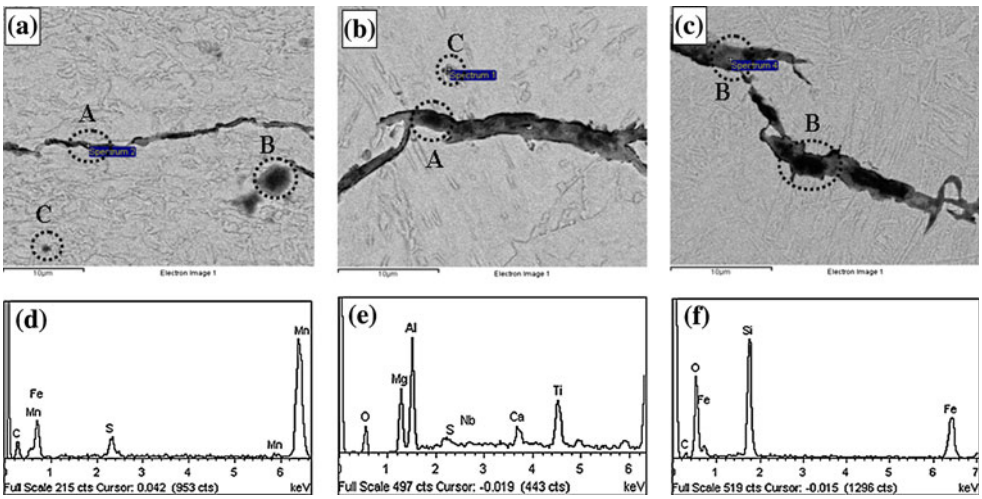

Fig. 6 BSE images of HIC for X80 steel of original (**a**), air cooling (**b**) and water quchening (**c**) and EDS on inclusions A (**d**), B (**e**) and C (**f**)

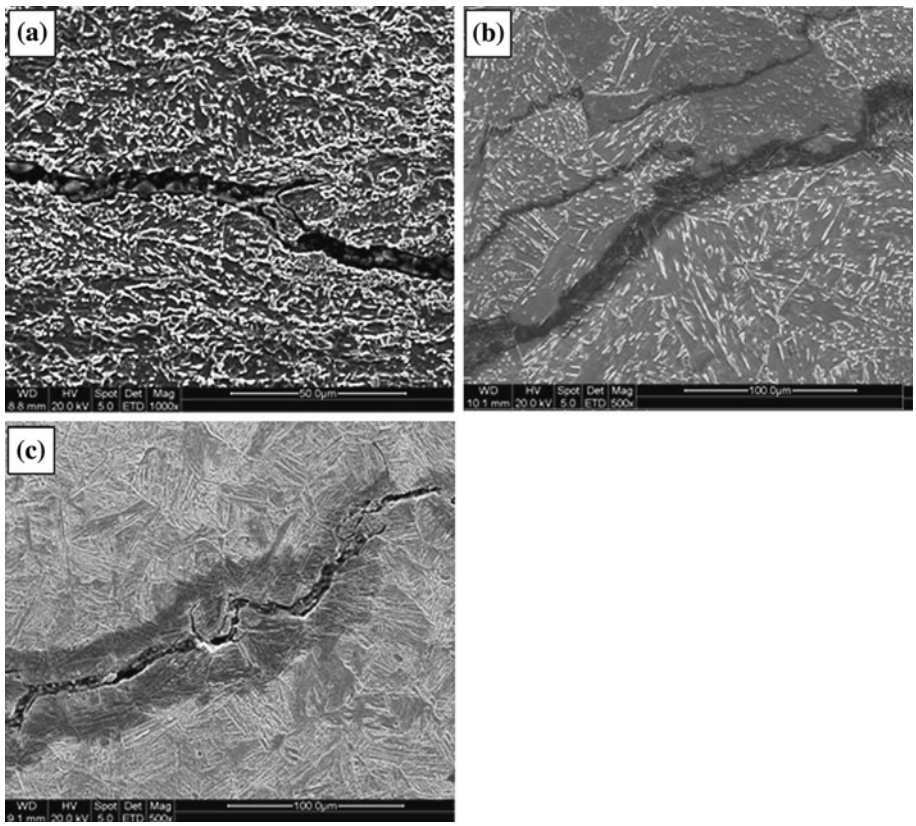

Fig. 7 SEM images showing HIC propagation path in the different microstructure X80 steels steel. **a** Original; **b** Air cooling; **c** Water quenching

around such inclusions [14]. Thus, no cracks are associated with inclusions enriched in Si.

HIC propagation path

Figure 7 shows HIC optical micrographs at the vertical section of the three specimens tested. It can be seen that the cracks in these specimens are typical stepwise cracks (SWC). For original and air cooled specimen, the dominant mode of crack propagation is transgranular cracking (Fig. 7a, b), while intergranular cracking, accompanied by little transgranular cracking, is the main mode of crack propagating in the water quenched specimen (Fig. 7c).

Conclusions

(1) The X80 steels with original or heat-treated microstructure used in this study all had good HIC resistance in wet H_2S environment, although the HIC susceptibility was larger for the steel with air cooled

or water quenched microstructure than for the steel with original microstructure.

(2) The ability of microstructure to trap hydrogen was explained in terms of the apparent diffusivity (D_{app}), permeability ($J_{\infty}L$), and solubility of hydrogen in steel (c_{app}). The lower the values of D_{app} and $J_{\infty}L$ and the larger the value of c_{app}, the more the hydrogen is entrapped in the steel and the larger the HIC susceptibility of the X80 steel.

(3) There were three types of inclusions in X80 steel. The inclusions rich in Mn and Al acted as the initiation sites for HIC cracking, and no HIC cracks were observed at inclusions rich in Si.

(4) The cracks in the steels are typical stepwise cracks (SWC), the dominant mode of crack propagation is transgranular propagation for the steels in the original and air cooled condition, while intergranualar propagation accompanied by a limited transgranular propagation is the main mode of crack propagation for the steel in the water quenched condition.

Acknowledgements This study was supported by China Postdoctoral Science Foundation (No: 20090450293) and China National Natural Science Foundation (No: 50971016).

References

1. Carneiro RA, Ratnapuli RC, Lins VFC (2003) Mater Sci Eng A 357(1–2):104
2. Sozanska M, Klyk-Spyra K (2006) Mater Charact 56(4–5):399
3. Hardie D, Charles EA, Lope AH (2006) Corros Sci 48(4):4378
4. Beidokhti B, Koukabi AH, Dolati A (2009) Mater Charact 60(3):225
5. Domizzi G, Anteri G, Ovejero-García J (2001) Corros Sci 43(2):325
6. Beidokhti B, Dolati A, Koukabi AH (2009) Mater Sci Eng A 507(1–2):167
7. Hara T, Asahi H, Ogawa H (2004) Corrosion 60(12):1113
8. Elboujdaini M, Sastri VS, Perumareddi JR (2006) Corrosion 62(1):29
9. Zhao MC, Shan YY, Xiao FR, Yang K, Li YH (2002) Mater Lett 57(1):141
10. Zhao MC, Yang K (2005) Scripta Mater 52(9):881
11. Park GT, Koh SU, Jung HG et al (2008) Corros Sci 50(7):1865
12. Du CW, Li XG, Liang P, Cheng YF (2009) J Mater Eng Perform 18(2):216
13. Liu ZY, Li XG, Du CW, Zhai GL, Cheng YF (2008) Corros Sci 50(8):2251
14. Liu ZY, Li XG, Du CW, Lu L et al (2009) Corros Sci 51(4):895
15. Kim WK, Koh SU, Yang BY, Kim KY (2008) Corros Sci 50(12):3336
16. Dong CF, Li XG, Liu ZY, Zhang YR (2009) J Alloys Compd 484(1–2):966
17. Zhao MC, Tang B, Shan YY, Yangc K (2003) Metall Mater Trans A 34(5):1089
18. Zhao MC, Yang K (2005) J Mater Res 20(9):2248
19. ISO 17081:2004(E). Method of measurement of hydrogen permeation and determination of hydrogen uptake and transport in metals by an electrochemical technique, ISO, Switzerland, 2004
20. Al-Anezi MA, Frankel GS, Agrawal AK (1999) Corrosion 55:1101
21. Fernandes M, Cheung N, Garcia A (2002) Mater Charact 48(4):255
22. Garet M, Brass AM, Haut C, Guttierez-Solana F (1998) Corros Sci 40(7):1073